J. Fluid Mech. (2004), *vol.* 501, *pp.* 149–168.
DOI: 10.1017/S0022112003007420 Printed in the United Kingdom

Development of particle dispersion characteristics from arbitrary initial conditions in isotropic turbulence

By DAVID I. GRAHAM

Department of Mathematics and Statistics, University of Plymouth, Drake Circus, Plymouth, Devon PL4 8AA, UK

(Received 22 August 2002 and in revised form 16 September 2003)

Discrete particles released into turbulent carrier flows respond to that turbulence over periods of time which depend on the particle inertia and the initial state of the particle. Due to the turbulence, the velocity of the particles becomes random and they will become dispersed throughout the carrier flow. The level of randomness of the particle velocities can be quantified by the particle kinetic stress and the spreading rate is characterized by the dispersion coefficient. In the idealized case of stationary isotropic turbulence, the kinetic stress and dispersion coefficients approach limiting values long after release. Previous analysis by the author has provided development times for dispersion coefficients and kinetic stress in cases where particles were released from a point source: (i) from an initial state of rest, and (ii) with kinetic stress identical to that found in the steady state. This paper generalizes the analysis by allowing for arbitrary initial particle velocity and displacement distributions. As with the previous analysis, the primary focus is on high-inertia particles. Unlike the previous work, however, the present analysis is applicable to the common practice in direct numerical simulations of setting initial particle velocities equal to local fluid velocities. Several different estimators of the particle dispersion coefficient are considered. Whereas each estimator leads to the same long-time value, the time taken to approach this value can vary dramatically. Expressions for development times are given for the particle kinetic stress and dispersion coefficients. Consequences of the analysis for experimental and computational studies are discussed.

1. Introduction

The dispersion of a discrete particulate phase due to random excitation by a turbulent carrier phase is important in industry and the environment. In industry, the phenomenon is important in pneumatic conveying, spray-drying, combustion and flow separation, to name but a few examples. In the environment, the spreading of automotive, industrial and domestic pollution is a major concern. It is well known that the turbulent dispersion is generally significantly greater than that due to molecular diffusion. It is therefore important in practice to quantify this dispersion so that models can be formulated for prediction of its consequences. Many of the models used in practice use suitably modified versions of Fick's law of diffusion. Recent examples include Binder & Hanratty (1991), Hanratty & Binder (1993) and Mols (1999). The dispersiveness of the particulates is then characterized by the *dispersion coefficient* or *dispersivity*.

Because of the importance of the phenomenon, many experimental and computational studies have tried to quantify dispersion. The general idea is to determine the dispersion in a relatively simple flow, and to use the resultant dispersion coefficients in numerical models of more relevant and complex flows. For example, Hinze (1975) discusses several experimental studies on the dispersion of tracers in turbulent pipe flows. Vames & Hanratty (1988) performed more recent experiments along the same lines. Snyder & Lumley (1971) and Wells & Stock (1983) measured the spread of solid particles released into a decaying grid turbulence. Karnik & Tavoularies (1989), Tavoularies & Karnik (1989) and Huang (1996) measured dispersion in a simple homogeneous shear flow.

Direct numerical simulation (DNS) techniques have also been used to avoid some of the experimental uncertainties in measuring dispersion. For example, Squires & Eaton (1991) and Elghobashi & Truesdell (1992) simulated dispersion in both decaying and forced isotropic flows.

Almost all of the experiments and computations mentioned above have been carried out for particles with relatively low inertia. A major reason for this is that measurements on high-inertia particles will be strongly dependent on the initial particle conditions. Experimentally, turbulence of high-inertia particles is unlikely to be able to develop sufficiently in confined laboratory spaces. Similarly, DNS and large-eddy simulation (LES) computations are very expensive and computations for large particles may not yet be economical. If measurements are carried out on large particles, an understanding of how well-developed the particle turbulence is likely to be, within physical or economic constraints, is essential. This is one motivation for the work presented in this paper, which investigates development time for various turbulence quantities of high-inertia particles.

A second motivation arises from the many Lagrangian models other than DNS and LES reported in the literature (see surveys by Stock 1996; Crowe, Troutt & Chung 1996; Graham 1998). An essential aspect of characterizing the performance of such models is to determine the long-time dispersivity of the model over a range of conditions (see Graham & James 1996; Launay 1998, for example). In particular, models are being developed to account for the 'inertia effect' where the dispersivity of high-inertia particles exceeds that of fluid elements in the absence of gravity (Reeks 1981). We also note the computations performed by Mei (1995), who used a simple particle dispersion model to confirm his analytical model of particle dispersion including nonlinear drag and history forces. For high-inertia particles, the model developer must be sure that the simulations have been running long enough for the particle turbulence to become very close to its long-time behaviour.

Before describing more fully the analysis carried out in this paper, it is useful to summarize the theoretical background for studies of particle dispersion. We start with molecular diffusion from a fixed point, which is governed by Fick's law:

$$\frac{\partial C}{\partial t} = D\nabla^2 C, \tag{1.1}$$

where C is the concentration and D is the diffusion coefficient. Einstein (1905) showed that

$$D = \langle X^2 \rangle / (2t), \tag{1.2}$$

with $\langle X^2 \rangle$ being the mean-squared particle displacement.

In the case of turbulent fluid flow, D as defined above is time-dependent and Fick's law does not hold in this form (Hanratty, Latinen & Wilhelm 1956). For homogeneous

turbulent flow, however, Batchelor (1948) showed that the concentration satisfies a form of Fick's law:

$$\frac{\partial C}{\partial t} = D_{ij}\frac{\partial^2 C}{\partial x_i \partial x_j}, \tag{1.3}$$

with the time-dependent diffusion tensor D_{ij} given by

$$D_{ij}(t) = \frac{1}{2}\frac{\mathrm{d}}{\mathrm{d}t}\langle X_i X_j \rangle. \tag{1.4}$$

Batchelor's work followed that of Taylor (1921), who related dispersion of marked fluid particles to the Lagrangian temporal auto-correlation of the fluid velocities:

$$\langle X^2 \rangle = \langle u_f'^2 \rangle \int_0^t \int_0^{t'} R_L(\tau)\,\mathrm{d}\tau\,\mathrm{d}t', \tag{1.5}$$

so that

$$D(t) = \langle u_f'^2 \rangle \int_0^t R_L(\tau)\,\mathrm{d}\tau, \tag{1.6}$$

where

$$R_L(\tau) = \frac{\langle u'_f(t)u'_f(t+\tau)\rangle}{\langle u_f'^2 \rangle} \tag{1.7}$$

is the Lagrangian velocity auto-correlation (which is assumed to be independent of t).

Most of the above analysis can be adapted for the case when the concentration in question is that of a *dispersed* phase in a turbulent carrier. Three different versions of the dispersion coefficient have been used in the literature: (i) the true dispersion coefficient, (1.4), used by Batchelor (1948), (ii) the 'effective' version, (1.2), used by Einstein (1905), and (iii) the 'pseudo'-dispersion coefficient (1.6), used by Taylor (1921). The most common method used in the literature is an approximation to find the true dispersion coefficient (1.4) by numerical differentiation of the mean-squared displacement. This method has been used by many researchers including both experimentalists such as Taylor (1954), Vames & Hanratty (1988), Snyder & Lumley (1971), Wells & Stock (1983) and numerical modellers including Squires & Eaton (1991) and Elghobashi & Truesdell (1992). Others, such as Govan (1989) and Graham & James (1996) have used the effective dispersion coefficient. Launay (1998) characterized dispersion using the pseudo-dispersion coefficient. We note that, of course, all three methods lead to the same value in the long-time limit.

If the long-time dispersivity is the goal of a study, experiments or computations must be run long enough for the quantities of interest to be close to the long-time values. Graham (1996) showed that the development time for the different estimates is sensitive to the initial conditions of the particles in question. Two cases of particles released from a point source were investigated previously. The first case was where the particles were initially static. The second looked at the case where the particle initial velocities were assumed to be 'fully developed'. Here, the initial particle velocities were random, from a zero-mean distribution with variance equal to that found in the long-time limit. Generally, of course, the excited particles developed more quickly. The analysis showed the use of the effective dispersion coefficient to be very inefficient for high-inertia particles in that development times were an order of magnitude higher than for the alternatives. Development times were also shown to be highly dependent on initial particle conditions. However, the analysis is not applicable in the case in

which the initial particle velocity is set equal to the local fluid velocity – common practice in DNS studies, for example.

The present paper extends the work reported previously by considering the case where the initial particle velocity and concentration distributions are arbitrary. Development times for particle turbulence characteristics will be derived. The general approach is similar to that used by Friedlander (1957). The above-mentioned common practice can be accommodated by the analysis. In § 2, expressions for the particle kinetic stress and for the true, effective and pseudo- dispersion coefficients are given. For each of these quantities, the focus is on the development times for high-inertia particles. The long-time behaviour for this limiting case is noted. In § 3, development times are investigated further and expressions are derived for the times required for the quantities of interest to develop to within a given tolerance of the long-time values. The repercussions of the analysis are discussed in § 4. Conclusions are presented in the final section.

2. Particle dispersion characteristics

In this paper, we restrict our attention to the motion of high-density particles for which the equation of motion is given by

$$\frac{\mathrm{d}u_p}{\mathrm{d}t} = \beta(u_f - u_p), \tag{2.1}$$

where u_p is the instantaneous particle velocity (in the x-direction), u_f is the instantaneous fluid velocity 'seen' by the particle and β is the reciprocal of the relaxation time scale of the particle, τ_p. In the analysis, we are primarily interested in high-inertia particles, for which the Stokes number is large (i.e. $\tau_p \gg \tau_{fp}$, so that $\beta\tau_{fp} = \tau_{fp}/\tau_p \ll 1$), where τ_{fp} is the integral scale of the fluid velocity 'seen' by the particles – see below. It will be shown that the quantities of interest here depend in general on the auto-correlation $\langle u'_f(t)u'_f(t+\tau)\rangle$ (where the angled brackets indicate ensemble-averaging) but that for high-inertia particles they are independent of the details of this expression. This means that no information is lost in considering only one spatial dimension. Accelerations due to gravity and other body forces are neglected here, for simplicity (though these can easily be included and the development times are unchanged from the present analysis). Without loss of generality, it can be assumed that the mean fluid velocity is zero.

We further assume that the viscous drag follows Stokes' law, so that β is a constant. In practice, of course, drag will be nonlinear, effectively decreasing particle response times. When gravity is important, the particle settling velocity will far exceed the turbulence intensity; thus we can define an effective particle relaxation time and this will be effectively constant. The linear analysis thus holds for this case and can predict transient behaviour. The analysis is not applicable only in the relatively unimportant case of nonlinear drag but zero gravity.

The solution to equation (2.1) is given by

$$u_p(t) = \mathrm{e}^{-\beta t}u_p(0) + \beta\int_0^t \mathrm{e}^{\beta(t'-t)}u_f(t')\,\mathrm{d}t'. \tag{2.2}$$

The mean velocity is given by averaging this equation:

$$\langle u_p(t)\rangle = \mathrm{e}^{-\beta t}\langle u_p(0)\rangle, \tag{2.3}$$

so that the particle fluctuating velocity is

$$u'_p(t) = u_p(t) - \langle u_p(t)\rangle = \mathrm{e}^{-\beta t}u'_p(0) + \beta\int_0^t \mathrm{e}^{\beta(t'-t)}u_f(t')\,\mathrm{d}t'. \tag{2.4}$$

The particle position at time t is therefore given by

$$\begin{aligned} x_p(t) &= x_p(0) + \int_0^t u_p(t')\,\mathrm{d}t' \\ &= x_p(0) + \frac{u_p(0)}{\beta}(1-\mathrm{e}^{-\beta t}) + \beta\int_0^t\int_0^{t''} \mathrm{e}^{\beta(t'-t'')}u_f(t')\,\mathrm{d}t'\,\mathrm{d}t''. \end{aligned} \tag{2.5}$$

The mean and fluctuating particle positions are thus given by

$$\langle x_p(t)\rangle = \langle x_p(0)\rangle + \frac{\langle u_p(0)\rangle}{\beta}(1-\mathrm{e}^{-\beta t}), \tag{2.6}$$

$$x'_p(t) = x'_p(0) + \frac{u'_p(0)}{\beta}(1-\mathrm{e}^{-\beta t}) + \beta\int_0^t\int_0^{t''} \mathrm{e}^{\beta(t'-t'')}u_f(t')\,\mathrm{d}t'\,\mathrm{d}t''. \tag{2.7}$$

The equations above are used as the basis of the remainder of this paper.

2.1. *Global particle kinetic stress $E(t)$*

Squaring $u'_p(t)$ and taking the ensemble average, we obtain

$$\begin{aligned} E(t) = \langle u'_p(t)^2\rangle = \mathrm{e}^{-2\beta t}\langle u'_p(0)^2\rangle + 2\mathrm{e}^{-2\beta t}\int_0^t \mathrm{e}^{\beta t'}\langle u_f(t')u'_p(0)\rangle\,\mathrm{d}t' \\ + \beta^2\mathrm{e}^{-2\beta t}\int_0^t\int_0^t \mathrm{e}^{\beta(t'+t'')}\langle u_f(t')u_f(t'')\rangle\,\mathrm{d}t'\,\mathrm{d}t''. \end{aligned} \tag{2.8}$$

If we assume that the initial particle velocity and the fluid velocity are uncorrelated, the second term in (2.8) vanishes. The third term is exactly the same as that arising if the initial particle velocity is zero (i.e. the case treated by Graham 1996). Eventually, therefore

$$E(t) = \langle u'_p(0)^2\rangle\mathrm{e}^{-2\beta t} + \frac{\beta}{2}\langle u'^2_f\rangle\int_0^t [2\mathrm{e}^{-\beta\tau} - \mathrm{e}^{-2\beta t}(\mathrm{e}^{\beta\tau}+1)]R_{fp}(\tau)\,\mathrm{d}\tau, \tag{2.9}$$

where $R_{fp}(\tau)$ is the auto-correlation of the fluid velocity seen by a particle. For high-inertia particles ($1/\beta \gg \tau_{fp}$), and long times ($t \gg 1/\beta$), this integral is independent of the form of $R_{fp}(\tau)$ and depends only on the associated integral time scale τ_{fp}. Equation (2.9) becomes

$$\begin{aligned} E(t) &= \langle u'_p(0)^2\rangle\mathrm{e}^{-2\beta t} + \langle u'^2_f\rangle\beta\tau_{fp}(1-\mathrm{e}^{-2\beta t}) \\ &= E_0\mathrm{e}^{-2\beta t} + \overline{E}(1-\mathrm{e}^{-2\beta t}), \end{aligned} \tag{2.10}$$

where $E_0 = \langle u'_p(0)^2\rangle$ is the initial value of the particle kinetic stress and $\overline{E} = \beta\tau_{fp}\langle u'^2_f\rangle$ is the long-time value of this quantity for high-inertia particles.

The above expression is consistent with the analysis given in Graham (1996) for the cases of initially static ($E_0 = 0$) and initially excited ($E_0 = \overline{E}$) particles. Note that this quantity is not the same as the local entity that would be measured by particle velocimetry. The *global* particle kinetic stress is given by ensemble-averaging over all particles at a given time. On the other hand, the *local* kinetic stress is an average over all particles *at a given point in space* at a given time. It is possible to analyse this using a p.d.f. approach, but that is beyond the scope of the present paper.

In order to test the validity of these expressions, simulations were carried out using a simple 'eddy interaction model' (Graham 1996). The underlying flow was isotropic turbulence with mean speed 0, Lagrangian integral time scale $\tau_L = 1$; 10 000 high-inertia computational particles ($\tau_p = 100$) were used. Using values of $k = 0$, 1, 2, 5 and 10, and considering t up to $5\tau_p$, the maximum relative error between predicted analytical values for $E(t)$ and computed numerical ones was less than 3.3%. This is within the 'error bars' of the computed values; thus the predictive value of the analytical expressions is excellent.

2.2. *Particle dispersion coefficient* $D(t)$

The particle dispersion coefficient is given by

$$D(t) = \frac{1}{2}\frac{\mathrm{d}}{\mathrm{d}t}\langle x'_p(t)^2\rangle = \langle u'_p(t)x'_p(t)\rangle. \tag{2.11}$$

Multiplying the expression for $u'_p(t)$ (2.4) by that for $x'_p(t)$ (2.7), ensemble averaging and simplifying the resulting integral gives

$$D(t) = \frac{1}{\beta}\mathrm{e}^{-\beta t}(1-\mathrm{e}^{-\beta t})E_0 + \int_0^t [1+\mathrm{e}^{\beta(-2t+\tau)} - \mathrm{e}^{-\beta t}(1+\mathrm{e}^{\beta\tau})]R_{pf}(\tau)\,\mathrm{d}\tau, \tag{2.12}$$

where we have again assumed that the initial particle velocity and the fluid velocity are uncorrelated. For small β and large t, this becomes

$$D(t) = E_0\frac{1}{\beta}\mathrm{e}^{-\beta t}(1-\mathrm{e}^{-\beta t}) + \overline{D}(1-\mathrm{e}^{-\beta t})^2, \tag{2.13}$$

where $\overline{D} = \langle u'^2_f\rangle\tau_{fp}$ is the long-time value of the particle dispersion coefficient.

Again, simulations were carried out using an eddy interaction model. Predicted values agreed with computed ones to within a few percent, again within the 'error bars' of the computed values. In this case, the main contributor to the error is the numerical differentiation of the dispersion. Again, therefore, the predictive value of the analytical expression for $D(t)$ is excellent.

2.3. *Effective dispersion coefficient* $D^{eff}(t)$

Dispersion coefficients are in practice often approximated by using the expression

$$D^{eff}(t) = \frac{1}{2t}\langle x'_p(t)^2\rangle, \tag{2.14}$$

which approaches the previous expression for the dispersion coefficient in the long-time limit. Forming the product $\langle x'_p(t)^2\rangle$ using equation (2.7) and simplifying after dividing through by $2t$ gives

$$D^{eff}(t) = \frac{1}{2\beta^2 t}\Bigg\{\beta^2 X_0^2 + E_0(1-\mathrm{e}^{-\beta t})^2 + \int_0^t \left[2(t-\tau) - \frac{1}{\beta}(2+\mathrm{e}^{-\beta\tau}+\mathrm{e}^{-\beta t}(2+\mathrm{e}^{-\beta\tau}+\mathrm{e}^{\beta\tau})+\mathrm{e}^{-2\beta t}\mathrm{e}^{-\beta\tau})\right]R_{pf}(\tau)\,\mathrm{d}\tau\Bigg\},$$

where X_0^2 is the initial variance of the particle displacement, and we have again assumed that the inter-correlations between the fluid velocity and initial particle velocity and displacement are zero. For $t \gg 1/\beta \gg \tau_{fp}$, the contribution from X_0^2 is negligible compared with that due to E_0 (i.e. the variance of the initial particle velocity is much more influential than that of the initial particle displacement). The effective

dispersion coefficient can then be approximated as

$$D^{eff}(t) = \frac{1}{2\beta^2 t}[E_0(1-\mathrm{e}^{-\beta t})^2] + \overline{D}\left[1 - \frac{1}{2\beta t}(1-\mathrm{e}^{-\beta t})(3-\mathrm{e}^{-\beta t})\right]. \tag{2.15}$$

Once again, equation (2.15) is consistent with the expressions given in Graham (1996).

Simulations to test the validity of the predictions were again carried out using an eddy interaction model, with the same details as previously. Computed values agreed to within 3% of the predicted values, again within the 'error bars' of the computed values.

2.4. *Pseudo-dispersion coefficient* $D^{ps}(t)$

Following Graham (1996), we define the 'pseudo-dispersion coefficient' to be the integral of the particle velocity auto-correlation. In practice, there are several alternative ways that one might define the pseudo-dispersion coefficient, namely

$$\text{(i)} \quad \int_0^{\infty} R_p(t,\tau)\,\mathrm{d}\tau,$$

$$\text{(ii)} \quad \int_0^{t} R_p(\tau)\,\mathrm{d}\tau,$$

$$\text{(iii)} \quad \int_0^{(1-\alpha)t} R_p(\alpha t,\tau)\,\mathrm{d}\tau,$$

where

$$R_p(t,\tau) = \langle u'_p(t)u'_p(t+\tau)\rangle \tag{2.16}$$

is the particle velocity auto-correlation and $R_p(\tau) = R_p(\infty,\tau)$ is its limiting form as $t \to \infty$.

Expression (i) is that used in Graham (1996) – it assumes that the value of the particle velocity correlation is known for an infinite range of times. Expression (ii) requires *a priori* knowledge of the particle velocity auto-correlation and is exactly equal to the true dispersion coefficient if $E_0 = \overline{E}$. In expression (iii), the total computation time is t, with a fraction α of this time used to develop the particle turbulence, the remainder being used to integrate the velocity auto-correlation. In practice, we are interested in the real cost of evaluating this form using finite computation times and without any assumptions on the form of the velocity correlations, so that we concentrate on expression (iii).

For small β and large t, the auto-correlation becomes

$$R_p(t,\tau) = E_0\mathrm{e}^{-\beta(2t+\tau)} + \overline{E}\mathrm{e}^{-\beta\tau}(1-\mathrm{e}^{-2\beta t}). \tag{2.17}$$

The pseudo-dispersion coefficient is then given by

$$\frac{1}{\beta}E_0\mathrm{e}^{-2\alpha\beta t}(1-\mathrm{e}^{-(1-\alpha)\beta t}) + \overline{D}(1-\mathrm{e}^{-(1-\alpha)\beta t})(1-\mathrm{e}^{-2\alpha\beta t}). \tag{2.18}$$

For this method, two questions now arise, namely what is the total time required for the computation and secondly what is the most efficient choice for α?

3. Development times for high-inertia particles

In this section, we investigate the time required for particles to acquire the dispersion characteristics mentioned previously. This follows the analysis given in Graham (1996), which demonstrated that initial conditions are highly influential in determining these

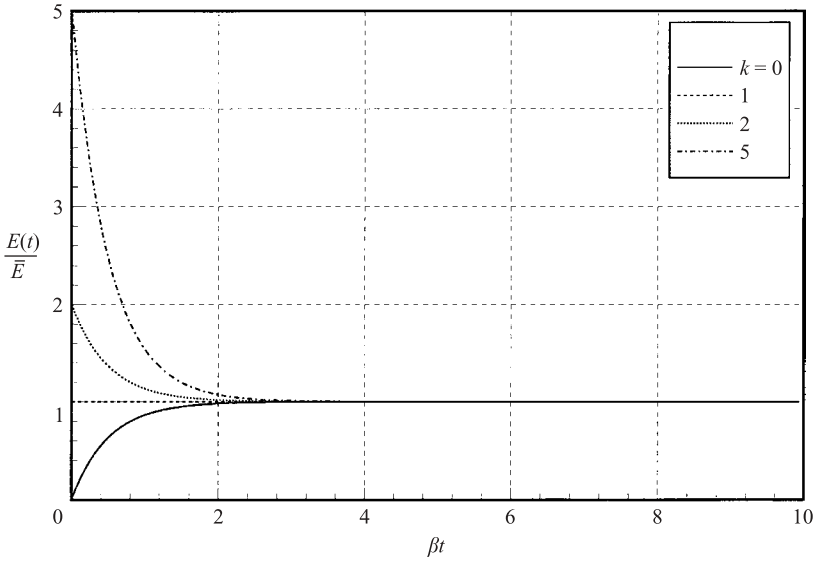

FIGURE 1. Normalized particle kinetic stress $E(t)/\overline{E}$ vs. βt.

development times. In general, the development times for initially static particles were found to be significantly longer than for the initially excited particles. A corollary of the previous analysis was that the effective dispersion coefficient (which is used frequently in numerical studies) was shown to be a very time-consuming method for determination of long-time particle dispersivity.

It was demonstrated that the pseudo-dispersion coefficient also developed more quickly than the true dispersion coefficient. Furthermore, the true dispersion coefficient will in practice be approximated by numerical differentiation, which may introduce extra uncertainties in stochastic approximations. On the other hand, the pseudo-dispersion coefficient as defined previously did not properly account for the finite time over which the particle velocity auto-correlation must be integrated in practice. However, the resulting numerical integration may be generally less susceptible to stochastic variation than numerical differentiation. It is therefore not clear which is the most efficient method for evaluating dispersion coefficients. This point is explored in § 4 of this paper.

We should note that many of the resulting expressions could be derived within the kinetic equation methodology of Reeks (1991). It could be argued that this method is more elegant than that adopted here. However, the present analysis, which develops quantities directly from the expressions for the particle velocity and displacement, has the advantage of simplicity and the amount of analytical effort in either case is similar.

3.1. *Global particle kinetic stress*

The development of the normalized particle kinetic stress $E(t)/\overline{E}$ is illustrated for different initial conditions in figure 1. In general, $E(t)$ is monotonic: if it is initially less than its long-time value, it increases towards its limit value and it correspondingly decreases towards its limit if it initially exceeds this limit. In the following, we are interested in the development time for this quantity, which is defined as the time required for the relative difference between $E(t)$ and its long-time limiting value E to lie within a specified tolerance ρ.

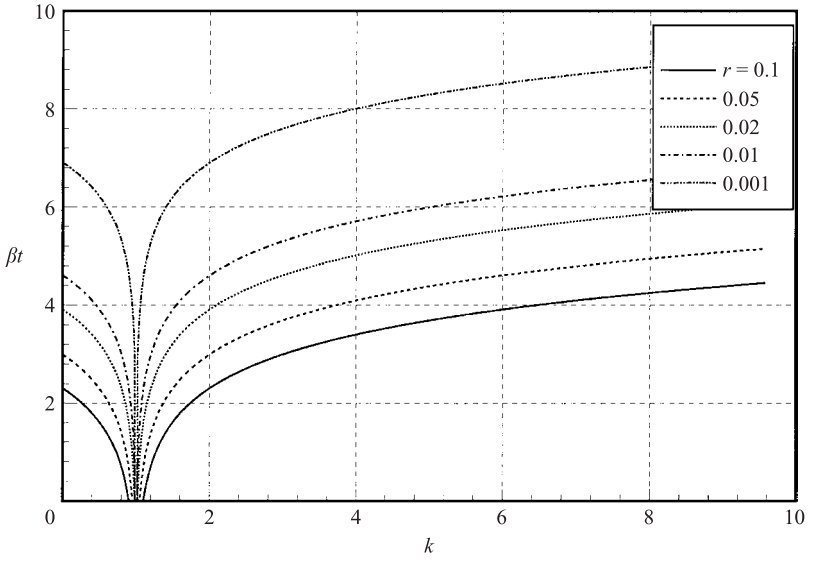

FIGURE 2. Development times: particle kinetic stress.

Equation (2.10) can be rearranged to give the relative error in the kinetic stress:

$$\frac{E(t)-\overline{E}}{\overline{E}} = (k-1)\mathrm{e}^{-2\beta t}, \tag{3.1}$$

where $k = E_0/\overline{E}$ is the ratio of initial to final particle kinetic stress. The development time can be expressed as the time required for the left-hand side of (3.1) to be equal to some predetermined tolerance level ρ. Beyond this time, the particle kinetic stress will always be within the allowed tolerance. The development time is given by

$$t_\rho = \frac{1}{2\beta}\ln\left(\frac{|k-1|}{\rho}\right). \tag{3.2}$$

Note that $E(t)$ either increases monotonically if $k < 1$ (i.e. the initial kinetic stress is less than the final value) or it decreases monotonically if $k > 1$. Negative solutions for the development time are also possible, in which case the development has 'already' occurred and the initial particle kinetic stress is within the required relative tolerance. Figure 2 illustrates the development times in terms of tolerance level plotted as a function of k. The symmetry about the line $k = 1$ illustrates that the development time for a given tolerance depends only on the difference between the initial particle kinetic stress and the long-time value.

Here, we have found the development time for the global kinetic stress (i.e. averaged over particles at all locations). It can be shown using a p.d.f. approach that the development time for the local kinetic stress is $1/2\beta\rho$. This is significantly greater than the time for the global kinetic stress to develop.

3.2. *Particle dispersion coefficient* $D(t)$

Whereas development of the particle kinetic stress is monotonic, the evolution of the dispersion coefficients is more complex. Figure 3 illustrates the development of the true dispersion coefficients (normalized with the long-time value $\overline{D}$) for the cases $k = 0, 1, 2, 3$ and 4 (where k is again defined as above as the initial normalized particle kinetic stress). For $k < 2$, the dispersion coefficient is monotonic. However, for k in

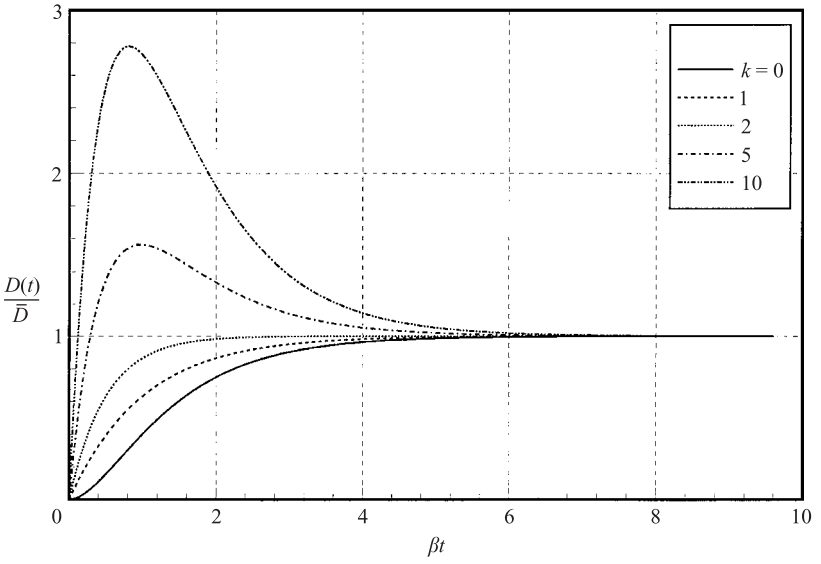

FIGURE 3. Normalized particle dispersion coefficient $D(t)/\overline{D}$ vs. βt.

excess of 2, the dispersivity grows from its initial value of zero, quickly exceeds its limiting value, grows to a maximum and then decays monotonically.

From equation (2.13), the relative error in the true dispersion coefficient is given by

$$\frac{D(t)-\overline{D}}{\overline{D}} = k\mathrm{e}^{-\beta t}(1-\mathrm{e}^{-\beta t}) - \mathrm{e}^{-\beta t}(2-\mathrm{e}^{-\beta t}). \tag{3.3}$$

The development time is then the solution of the above equation, with the left-hand side set equal to $\pm\rho$:

$$\pm\rho = \mathrm{e}^{-\beta t}(k-2) + \mathrm{e}^{-2\beta t}(1-k). \tag{3.4}$$

Substituting $y = \mathrm{e}^{-\beta t}$ we obtain a quadratic:

$$\pm\rho = y(k-2) + y^2(1-k), \tag{3.5}$$

which has the solution

$$y = \begin{cases} \left(\dfrac{2-k}{2(1-k)}\left(1 \pm \left(1 \pm 4\rho\dfrac{(1-k)}{(k-2)^2}\right)^{1/2}\right)\right), & k \neq 1, k \neq 2, \\ \rho, & k = 1, \\ \rho^{1/2}, & k = 2. \end{cases} \tag{3.6}$$

Clearly, y in equation (3.6) must be in the range $0 < y \leqslant 1$. In order to determine which of the possible solutions to use, we now investigate equation (3.4) fully.

For $0 \leqslant k \leqslant 2$ the normalized dispersion coefficient never exceeds unity and thus we use $-\rho$ (corresponding to the lower tolerance level) in the expression for the development time. For $k > 2$, there is a local maximum at $t = (1/\beta)\ln(2(1-k)/(2-k))$, at which the dispersion coefficient takes the value

$$\frac{k^2}{4(k-1)} > 1. \tag{3.7}$$

Two possibilities exist. The first is that the maximum value attained by the dispersion coefficient never exceeds the maximum tolerance level $+\rho$ so that the normalized

dispersion coefficient $D(t)/\overline{D}$ always lies within the tolerance after it has first reached this level. This is equivalent to the condition

$$\rho \geqslant \frac{(k-2)^2}{4(k-1)}. \tag{3.8}$$

Here, the negative square root is taken in the expression for the development time.

Otherwise, $D(t)/\overline{D}$ crosses the tolerance boundaries at three different times, twice 'on the way up' as it climbs to its maximum, and finally on the way back down, having attained its maximum (see figure 3). In this case, the development time should be taken as the largest of the three times given by the roots of equation (3.4).

To summarize, the development time is determined as

$$t_\rho = \begin{cases} \dfrac{1}{\beta}\ln\left(\dfrac{2(1-k)}{(2-k)(1-(1-4\rho(1-k)/(k-2)^2)^{1/2})}\right), & 0 \leqslant k \leqslant 2,\ k \neq 1, 2 \text{ or } k \geqslant 2, \\ & \quad \rho \geqslant \dfrac{(k-2)^2}{4(k-1)}, \\ \dfrac{1}{\beta}\ln\left(\dfrac{1}{\rho}\right), & k = 1, \\ \dfrac{1}{2\beta}\ln\left(\dfrac{1}{\rho}\right), & k = 2 \\ \dfrac{1}{\beta}\ln\left(\dfrac{2(1-k)}{(2-k)(1-(1+4\rho(1-k)/(k-2)^2)^{1/2})}\right), & k \geqslant 2,\ \rho < (k-2)^2/4(k-1), \end{cases} \tag{3.9}$$

Note that, for small ρ, the development time is

$$t_\rho = \begin{cases} \dfrac{1}{\beta}\ln\left(\dfrac{|k-2|}{\rho}\right), & k \neq 2, \\ \dfrac{1}{2\beta}\ln\left(\dfrac{1}{\rho}\right), & k = 2. \end{cases} \tag{3.10}$$

Figure 4 illustrates the development times for the true dispersion coefficient as a function of k and the magnitude of the tolerance, ρ. For low tolerances, there is a sharp minimum development time corresponding to $k = 2$. For higher tolerances, the minimum is less sharp and shifts towards higher values of k. The minimum in each case corresponds to the situation where the initial particle conditions are such that the maximum dispersivity is only just within the tolerance level. Any increase in the initial particle kinetic stress takes the maximum dispersivity outside the allowed range, which corresponds to the second possibility mentioned above. This explains the large jump in development times beyond the minimum values.

3.3. *Effective dispersion coefficient* $D^{eff}(t)$

The development of the normalized effective dispersion coefficient is illustrated for various initial particle conditions in figure 5. Again, the development is rather complex. The effective dispersivity increases monotonically for small values of the initial particle kinetic stress. For large values of E_0, the dispersivity increases from its initial value of zero, reaches a maximum and then decreases towards its long-time value.

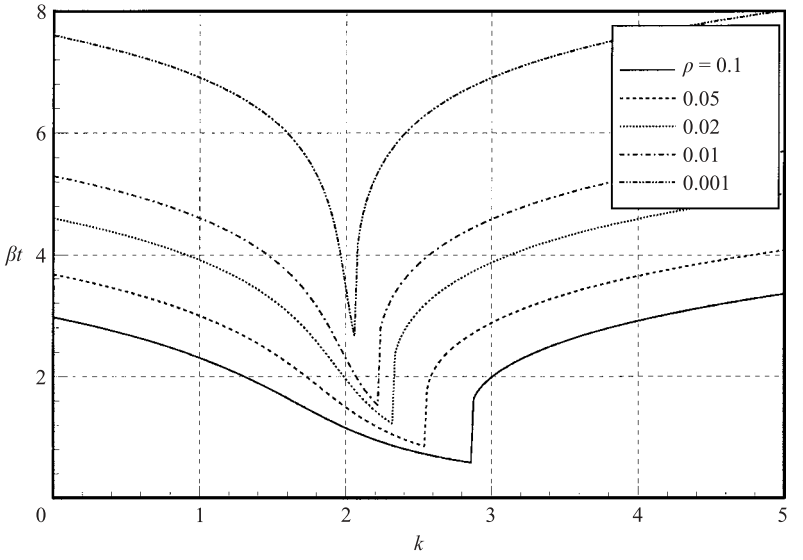

FIGURE 4. Development times: particle dispersion coefficient.

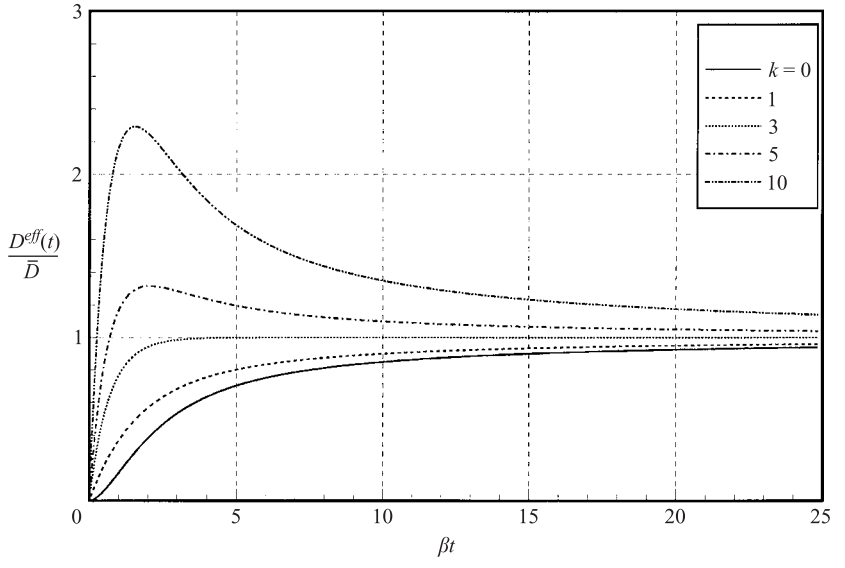

FIGURE 5. Normalized effective particle dispersion coefficient $D^{eff}(t)/\overline{D}$ vs. βt.

Equation (2.15) can be written in the form

$$\frac{D^{eff}(t)-\overline{D}}{\overline{D}} = \frac{1}{2\beta t}\left[\frac{E_0}{\overline{E}}(1-\mathrm{e}^{-\beta t})^2 - (1-\mathrm{e}^{-\beta t})(3-\mathrm{e}^{-\beta t})\right], \tag{3.11}$$

where we have again used the fact that $\overline{E} = \beta\overline{D}$ for heavy particles. Setting the left-hand side of (3.11) to a tolerance level of $\pm\rho$, this equation becomes

$$\pm\rho = \frac{1}{2\beta t}k(1-\mathrm{e}^{-\beta t})^2 - (1-\mathrm{e}^{-\beta t})(3-\mathrm{e}^{-\beta t}) \tag{3.12}$$

(where k is again defined as the normalized initial particle kinetic stress).

Closed-form solutions are not generally available for this equation. Note however that, for small ρ, development times are large compared with $1/\beta$. This means that the exponential terms can be neglected and the development time is then simply

$$t_\rho = \frac{1}{2\beta\rho}|k-3|. \tag{3.13}$$

Note that this expression appears to show that the effective dispersion coefficient is immediately 'fully developed' when $k=3$. This is not in fact the case and the development time here is the solution of

$$\rho = \frac{2}{\beta t}\mathrm{e}^{-\beta t}(1-\mathrm{e}^{-\beta t}). \tag{3.14}$$

The solutions to this equation must be approximated numerically. For completeness, note that development times for tolerances of 0.1, 0.05, 0.01, 0.005, 0.001 and 0.0001 are $2.12/\beta$, $2.64/\beta$, $3.91/\beta$, $4.48/\beta$, $5.83/\beta$ and $7.84/\beta$, respectively. Clearly, a graph of development time βt versus k (not shown here) would show a set of straight lines through $k=3$, $\beta t=0$, with slope equal to $1/(2\rho)$.

3.4. *Pseudo-dispersion coefficient* $D^{ps}(t)$

When the upper limit of integration of the particle velocity auto-correlation is infinite, the time development of the pseudo-dispersion coefficient is identical to the particle kinetic stress, i.e. it is monotonic for all initial conditions and development times are again given by equation (3.2).

When the finite integration time for evaluation of the particle auto-correlation is taken into account, however, a much more complex picture emerges. The pseudo-dispersion coefficient is given by

$$\frac{D^{ps}(t)-\overline{D}}{\overline{D}} = \left(\frac{E_0}{\overline{E}}-1\right)\mathrm{e}^{-2\alpha\beta t}(1-\mathrm{e}^{-(1-\alpha)\beta t}) - \mathrm{e}^{-(1-\alpha)\beta t}. \tag{3.15}$$

Setting the left-hand side of this expression equal to $\pm\rho$, we obtain the equation

$$\pm\rho = (k-1)\mathrm{e}^{-2\alpha\beta t}\left(1-\mathrm{e}^{-(1-\alpha)\beta t}\right) - \mathrm{e}^{-(1-\alpha)\beta t}, \tag{3.16}$$

where k is as defined previously.

Contour plots characterizing the time required for development of the solution are given as functions of α in figure 6(*a–d*). The contours show the times at which $|D_{ps}(t)-\overline{D}|/\overline{D}$ reaches values of $\rho=0.1, 0.01$ and 0.001, for $0<\alpha\leqslant 1$. For $k<2$, $D^{ps}(t)$ never reaches its long-time value $\overline{D}$. For $k>2$, $D^{ps}(t)$ can exceed the long-time value, depending on the value of α.

The behaviour in several sections of the contour plot can be analysed. For $\alpha \ll 1/3$ and $t \gg 1$, the contours are described well by the relationship

$$t = \frac{\ln(\rho)}{\beta(\alpha-1)}, \tag{3.17}$$

independently of k.

For $\alpha \gg 1/3$ and $t \gg 1$, the contours are given by

$$t = \frac{1}{2\beta\alpha}\ln\left(\frac{|k-1|}{\rho}\right), \quad k\neq 1. \tag{3.18}$$

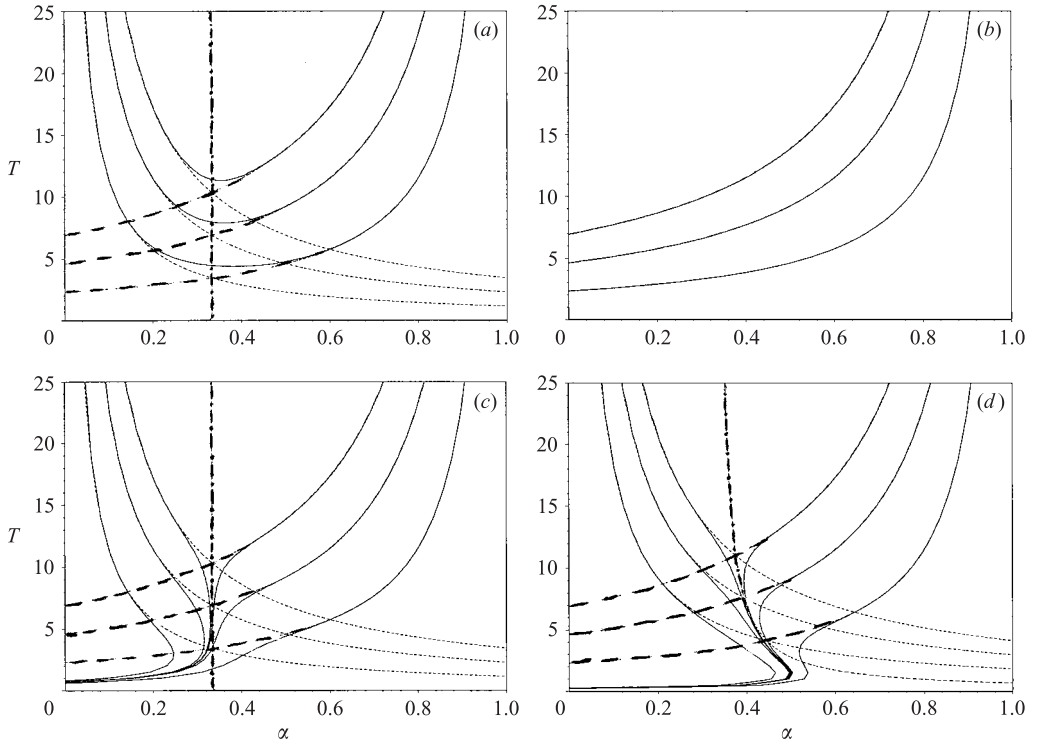

FIGURE 6. Development times: pseudo-particle dispersion coefficient: solid lines: solutions to equation (3.16); dotted lines: equation (3.17); dashed lines: equation (3.18); dot-dashed lines: equation (3.20). (*a*) $k = 0$, (*b*) $k = 1$, (*c*) $k = 2$, (*d*) $k = 10$.

For a given tolerance ρ, these two curves intersect at the point

$$\left.\begin{aligned} \alpha &= \begin{cases} \dfrac{\ln(|k-1|/\rho)}{\ln(|k-1|/\rho^3)}, & k \neq 1, \\ 0, & k = 1, \end{cases} \\ t &= \frac{1}{2\beta}\ln(|k-1|/\rho^3|). \end{aligned}\right\} \tag{3.19}$$

These points lie on a curve defined by the relationship

$$t = \frac{\ln(|k-1|)}{\beta(3\alpha - 1)}. \tag{3.20}$$

From figure 6(*a–d*), it is clear that the point of intersection provides, for given k and ρ, reasonable estimates of both the best value of α and the time t_ρ required for the solution to develop to within the required tolerance. Development times are underestimated using this method unless the initial particle stress exceeds the long-time value (i.e. unless $k > 1$). For $k > 1$, the method slightly overestimates the development times. In general, however, the time given by equation (3.19) is a reasonable estimate of the true development time, particularly for low tolerances. Note also that, for $k > 2$, $D^{ps}(t)$ is exactly equal to its long-time value for the value of α in (3.19).

The relationship (3.20) is not valid for $k = 1$ of course. In this case, the initial particle kinetic stress is exactly equal to its long-time value. Here, the particle turbulence itself

clearly takes no time to develop and all of the computational effort must go into the integration of the auto-correlation (i.e. choose $\alpha = 0$). The development time is then equal to $(1/\beta)\ln(1/\rho)$.

This discussion leads eventually to a much simpler way of looking at the problem. The time t_1 required for the auto-correlation to develop is $t_1 = (1/2\beta)\ln(|k-1|/\rho)$. In addition, extra time t_2, equal to $(1/\beta)\ln(1/\rho)$ is required to integrate the auto-correlation. The total computation time can thus be written as

$$t_\rho = \begin{cases} \dfrac{1}{2\beta}\ln\left\{\dfrac{|k-1|}{\rho} + \dfrac{1}{\beta}\ln(1/\rho)\right\}, & k \neq 1 \\ \dfrac{1}{\beta}\ln(1/\rho), & k = 1. \end{cases} \tag{3.21}$$

For $k < 1$, both the particle turbulence and the numerical integration time are under-developed so that this expression slightly underestimates the true development time. For $k > 1$, the particle turbulence is over-developed and the numerical integration under-developed, the net result being that the pseudo-dispersion coefficient is exactly equal to its final value. For $k < 2$, $D^{ps}(t)$ subsequently increases within the tolerance before finally decreasing towards the long-time limit. For $k > 2$, $D^{ps}(t)$ subsequently decreases within the tolerance before finally increasing towards the long-time limit. Development times from equation (3.21) are identical in form to those illustrated in figure 2 except that they must be shifted upwards by an amount equal to $(1/\beta)\ln(1/\rho)$.

The development times for this quantity are greater than for the true dispersion coefficient but significantly lower than for the effective dispersivity. As noted above, however, the use of numerical integration may mean that it is subject to more variation than the true dispersivity, which must be estimated in practice using numerical differentiation. The optimal choice (i.e. the fastest developing subject to acceptable variability) between true and pseudo- dispersivities could be determined by also finding the variance of these quantities as functions of time (rather than finding only the mean value as here). However, that is beyond the scope of this paper.

4. Discussion

In this section, we investigate the consequences of the foregoing analysis. First, we discuss the repercussions for experimental studies. Then we look at two distinct kinds of numerical simulation. The first kind is DNS computations whose purpose is to detect and predict new phenomena. Then we consider particle dispersion models whose purpose is either to mirror known behaviour in special cases so that they can be used with confidence in more realistic and complex flows or to confirm analytical predictions.

Unsurprisingly, the most popular method of evaluating dispersion coefficients in experiments is to use the *true* dispersion coefficient. In practice, this entails numerical differentiation of the mean-squared displacement (or, equivalently, estimating the slope of the graph of $X_p^2(t)$ against t). As mentioned in the introduction, most experimental studies are restricted to low-inertia particles, which respond rapidly to the fluid turbulence. It is easy to see why experimentalists have not generally used heavier particles. Hutchinson, Hewitt & Dukler (1971) estimated the turbulent eddy time scale in the flow through a pipe of radius R as $t_d = 0.35R/u*$. Hinze (1975) uses the data from Laufer (1954) to show that $u*/U$, the ratio of the friction velocity to the maximum mean velocity is around 0.035 for a Reynolds number of

500 000. Thus, for a 20 m s^{-1} turbulent air flow in a 10 cm pipe, t_d is roughly 0.05 s. A particle with a relaxation time τ_p of 0.5 s would be 'heavy', having a Stokes number $\beta = 1/10$. Starting such particles from rest, it would take a distance of approximately $U\tau_p \ln(2/0.05) \cong 37$ m for the true dispersion coefficient to develop. For heavier particles, or with less controlled initial conditions, development lengths would be still greater.

In the case of pipe flow, it is likely that by the time the dispersion coefficient is fully developed, many of the particles will have been affected by pipe–wall collisions. For example, for the above particle, the dispersion coefficient is developed to within 95% of its long-time value at around $3.7\tau_p$. At this time, the dispersion (i.e. the mean-squared displacement) is about 0.5 m^2 s^{-2} thus giving a root-mean-square displacement of about 7 cm. Since this is greater than the radius of the pipe, pipe–wall collisions can be expected to have been important well before this time.

Numerical experiments are less subject to such constraints than their physical counterparts. Thus, although the idealized case of stationary isotropic turbulence considered cannot be realized physically, it remains an important idealized test case, both for numerical experiments using DNS or LES and also for calibrating new multiphase flow models. Recent DNS studies of isotropic turbulence include those of Boivin, Simonin & Squires (1998), Sundaram & Collins (1999) and Ferrante & Elghobashi (2003). Although these authors primarily consider turbulence modulation effects rather than dispersion, some general observations can be made on the influence of the initial conditions. Some observations on the DNS results of Squires & Eaton (1991) and Elghobashi & Truesdell (1992) are made below.

Squires & Eaton (1991) and Elghobashi & Truesdell (1992) have computed dispersion coefficients of solid particles in decaying and forced isotropic turbulence. Squires & Eaton used particles with Stokes number $1/\beta\tau_{fp}$ up to 3.72 in decaying turbulence. The Stokes numbers for Elghobashi & Truesdell were generally less than 1. Several interesting points can be made by looking at the results. The first point is that the initial particle velocities are set equal to the velocities of the surrounding fluid. This appears to be standard practice, since it was also adopted by Boivin *et al.* (1998), Sundaram & Collins (1999) and Ferrante & Elghobashi (2003). However, it does not appear to be best practice. For $\beta\tau_{fp} = 1/3.72$ (the highest-inertia particles used by Squires & Eaton (1991)) this means that E_0 is about 3.72 times $\overline{E}$. This initial high kinetic stress is difficult for the particle to shake off. The most efficient choice for computations, given that particle kinetic stress and dispersion coefficients were both of interest, would be to set the initial particle kinetic stress equal to its long-time value. This could be achieved by setting the initial particle velocity to $1/3.72^{1/2}$ times the surrounding fluid velocity. If turbulence modulation is the main topic of interest, or if the long-time particle kinetic stress is not known, a better choice would be to set the particle velocity equal to the local mean velocity, which should be known *a priori*.

The second point to be made regarding these computations is that both pairs of authors use the mean-squared slip velocity $v_{rel}^2(t)$ to test the development of the particle turbulence. This approach was also adopted by Sundaram & Collins (1999). In particular, the time at which this quantity reaches a maximum is taken to be the time at which the particles had 'adjusted to the decaying turbulence'. Expressed in terms of multiples of particle time constant, however, the location of this maximum tends to zero for higher-inertia particles. Thus the particles are only beginning to respond to the turbulence at this time, and a much greater time is required for the particles to fully respond.

When the initial particle velocity is set equal to the local fluid velocity, the mean-squared slip velocity develops much more quickly than the dispersion coefficients. Suppose that K is the ratio of the initial mean-squared particle velocity to the mean-square of the fluid velocity fluctuations. It can be shown that the time for this quantity to develop within a tolerance of ρ of its long-time value is $\ln(K/\rho)/(2\beta)$. When the initial particle velocity is set equal to the local fluid velocity, K is unity. The development time for $v_{rel}^2(t)$ is then $\ln(1/\rho)/(2\beta)$, i.e. $5\tau_{fp}\ln(1/\rho)$ for a heavy particle with $\beta\tau_{fp} = 1/10$. For such a particle, the initial condition would mean a value of $k = E_0/\overline{E} = 10$. Development times for the particle kinetic stress and dispersion coefficient would then be $5\tau_{fp}\ln(8/\rho)$ and $10\tau_{fp}\ln(9/\rho)$, respectively. Thus, while $v_{rel}^2(t)$ develops to within a tolerance of 0.05 of its long-time value within 15 s, the corresponding development times for the particle kinetic stress and dispersion coefficient are 25 s and 52 s, respectively. It can therefore be misleading to base judgements of particle turbulence development on the progress of $v_{rel}^2(t)$.

Other features of the results can also be explained. For example, the 'overshooting' of the dispersion coefficients in Squires & Eaton figures 9 and 13, and for the uranium particles in figure 12(*b*) of Elghobashi & Truesdell is possibly due to too much particle kinetic stress at the beginning of the computations. The form of the curves is similar to figure 3 in the present paper, and even though the Elghobashi & Truesdell particles were of relatively low-inertia, similar behaviour is seen when substituting appropriate values in equation (2.12) above. An important consequence of this is that, since the dispersion coefficients in Squires & Eaton are not fully developed, their conclusion that "the dispersion of particles ... is greater than that of fluid elements" may not be valid in the long-time limit.

As mentioned above, calibration of numerical models by considering their performance in isotropic turbulence is an important part of model validation. Typically, this requires that models are capable of simulating the three main effects predicted from analysis: 'crossing trajectories' – reduced dispersion under gravity; 'inertia' – enhanced dispersion for heavy particles without gravity; and 'continuity' – different dispersivities in directions parallel and perpendicular to gravitational drift (see the discussion in Graham 1998, for example). Unfortunately, there is no standard approach for choosing development times and this means that the performance of some models can be misinterpreted.

Recent examples of calibrating numerical methods by considering isotropic turbulence include Wang & Stock (1992), Lu, Fontaine, & Aubertin (1993), Huang (1996), Graham & James (1996) and Launay (1998). A variety of approaches, both to computing diffusivities and to judging 'particle turbulence development', is used in these papers.

Wang & Stock (1992) were interested in tracer particles and thus needed no time for the particle kinetic stress to develop. They compared analytical and numerically predicted velocity auto-correlations. Lu *et al.* (1993) calculated dispersion coefficients using a time-series model. Their development time was about 1.4 s (i.e. the time taken for particles with an average speed of $0.66\,\mathrm{m\,s^{-1}}$ to travel 0.9 m). However, their heaviest particles had a time constant of 1.6 s. Having started the particles with the same velocity as the fluid, this means that the particles did not have time to shake off the initial conditions. The fact that the dispersion coefficient is not fully developed is evident from the curvature in their dispersion curve (figure 12). Again, this casts doubt upon the validity of their long-time dispersivity values for the heaviest particles.

Graham & James (1996) calculated the dispersivities produced by eddy-interaction model predictions over a range of Stokes numbers. For their heaviest particles

($\beta = 1/10$), it is clear (their figure 3) that the dispersion coefficients were still developing. The *effective* version of the dispersion coefficient was used. It is also apparent from their results (their figures 1 and 2) that particle dispersion coefficients were still in the process of developing. For the Graham & James (1996) results, computations were allowed to run for a duration of $1000\tau_L \approx 1000\tau_{fp}$, having begun with static particles. Using the present analysis, it can be seen that the resulting dispersion coefficients for the heaviest particles can be expected to be around 98.5% of the true long-time values at this time. Such computations are very expensive computationally. The cost can be greatly reduced by choosing the appropriate method of computing dispersion coefficients and setting the most beneficial initial conditions. For example, the *true* dispersion coefficient for the Graham & James computations would have developed to the same extent within $42\tau_L$, if the initial particle kinetic stress was set equal its long-time value. This time could be halved by setting $E_0 = 2\overline{E}$. This represents a huge reduction in computation times – a factor of almost 50.

Huang (1996) used both Monte Carlo and random Fourier models in both isotropic flow and in a simple turbulent shear flow. In her Monte Carlo simulations, the initial particle velocity is set equal to the instantaneous fluid velocity. The flow is then allowed to develop for an unspecified time and then dispersion coefficients are calculated using a numerically differentiated true dispersion coefficient. The computed values were higher than the predicted values. Again, this is possibly due to an initial excess in the particle kinetic stress.

Launay (1998) used both an eddy-interaction model and a generalized Markov chain model to compute dispersion coefficients. She used the pseudo-dispersion coefficient, and allowed about 1 s for the particle turbulence to develop, and a further 4 s to integrate the velocity auto-correlation (private communication, 1999). The heaviest particles in her computations had a time constant of roughly 1 s. The characteristic 'tailing-off' of the dispersion coefficients for high-inertia particles in Huang's figures I-5 and II-9 indicates that the particle turbulence is still developing at the end of the computations. Having started the computations with particles at rest, the particle kinetic stress (and hence the velocity auto-correlation) is only around 86% of its long-time value. A development time of 1.5 s would raise this to 95%. To compensate, less time (3 s should have been sufficient) could have been spent on the integration of the particle velocity auto-correlation. In this way, the computations could have been completed in 4.5 s, giving dispersion coefficients within a tolerance of 5%.

Finally, we note that evaluating dispersivities by visual inspection or numerical differentiation from graphs of mean-squared particle location against time has been commonplace (Snyder & Lumley 1971; Wells & Stock 1983; Lu *et al.* 1993; for example). Whilst this is reliable for low-inertia particles, the curvature (i.e. the derivative of the true dispersion coefficient) could be sufficiently small over a large range of times for high-inertia particles to lead to misinterpretation of the results. The net effect would be to misjudge dispersion coefficients for heavier particles (i.e. overpredict if $k < 2$ and underpredict otherwise).

5. Conclusions

This paper has investigated the influence of the initial velocity and displacement distributions on dispersion characteristics of high-inertia particles in homogeneous turbulence. The key dimensionless quantity characterizing development times is $k = E_0/\overline{E}$, the ratio of the initial particle kinetic stress to its long-time value. The influence of the initial displacement distribution of the particles is less important. The results of

the analysis have been used to interpret results from numerical studies. The following conclusions can be drawn.

(*a*) For the high-inertia particles, development times are proportional to the particle relaxation time.

(*b*) Development of the particle kinetic stress $E(t)$ is monotonic: increasing if initially less than the long-time value, and decreasing otherwise.

(*c*) Development of the true dispersion coefficient $D(t)$ is non-monotonic for particles with high initial kinetic stress. In this case, the dispersion coefficient can increase to well above its long-time value before decreasing towards its limiting value.

(*d*) Development of the effective dispersion coefficient $D_{eff}(t)$ exhibits similar non-monotonic behaviour. Development times, however, are much greater than for the true dispersion coefficient.

(*e*) Development times for $D_{ps}(t)$ slightly exceed those for $E(t)$ and $D(t)$, but are significantly less than those for $D_{eff}(t)$.

(*f*) The standard practice of setting initial particle velocities equal to instantaneous fluid velocities in DNS can be inefficient – a better choice would be to set particle velocities equal to local mean fluid velocities.

(*g*) The common practice of evaluating the 'mean-squared slip velocity' to determine whether flows have developed sufficiently can be misleading since this quantity can develop much more quickly than other particle quantities.

REFERENCES

Batchelor, G. K. 1948 Diffusion in a field of homogeneous turbulence. *Austral. J. Sci. Res.* A **2**, 437–450.

Binder, J. L. & Hanratty, T. J. 1991 A diffusion model for droplet deposition in gas/liquid annular flow. *Intl J. Multiphase Flow* **17**, 1–11.

Boivin, M., Simonin, O. & Squires, K. D. 1998 Direct numerical simulation ot turbulence modulation by particles in isotropic turbulence. *J. Fluid Mech.* **375**, 235–263.

Crowe, C. T., Troutt, T. R. & Chung, J. N. 1996 Numerical models for two-phase turbulent flows. *Annu. Rev. Fluid Mech.* **28**, 11–43.

Einstein, A. 1905 On the movement of small particles suspended in a stationary liquid demanded by the molecular-kinetic theory of heat. In *Einstein (1956) Investigations on the Theory of the Brownian Movement*. Dover Publications edition of 1926 translation.

Elghobashi, S. E. & Truesdell, G. C. 1992 Direct simulation of particle dispersion in a decaying isotropic turbulence. *J. Fluid Mech.* **242**, 655–700.

Ferrante, A. & Elghobashi, S. 2003 On the physical mechanisms of two-way coupling in particle-laden isotroci turbulence. *Phys. Fluids* **15**, 315–329.

Friedlander, S. K. 1957 Behavior of suspended particles in a turbulent fluid. *AIChE J.* **3**, 381–385.

Govan, A. H. 1989 A simple equation for the diffusion coefficient of large particles in a turbulent gas flow. *Intl J. Multiphase Flow* **15**, 287–294.

Graham, D. I. 1996 Dispersion of initially-static and initially-excited particles in a turbulent fluid flow. *Intl J. Multiphase Flow* **22**, 1005–1021.

Graham, D. I. 1998 Analytical comparison of Lagrangian particle dispersion models. *Paper 125, ICMF'98, Lyon, France.*

Graham, D. I. & James, P. W. 1996 Turbulent dispersion of particles using eddy interaction models. *Intl J. Multiphase Flow* **22**, 157–175.

Hanratty, T. J. & Binder, J. L. 1993 Use of Lagrangian statistics to describe turbulent dispersed flows. In *Particulate Two-Phase Flow*, Butterworth-Heinemann.

Hanratty, T. J., Latinen, G. & Wilhelm, R. H. 1956 Turbulent diffusion in particulately fluidized beds of particles. *AIChE J.* **2**, 372–380.

Hinze, J. O. 1975 *Turbulence*. McGraw Hill.

Huang, X. 1996 Turbulent dispersion of particles in a homogeneous uniform shear. PhD thesis, Washington State University, USA.

Hutchinson, P., Hewitt, G. F. & Dukler, A. E. 1971 Deposition of liquid or solid dispersions from turbulent gas streams: a stochastic model. *Chem. Engng Sci.* **26**, 419–439.

Hyland, K. E., McKee, S. & Reeks, M. W. 1999 Exact analytic solutions to turbulent particle flow equations. *Phys. Fluids* **11**, 1249–1261.

Karnik, U. & Tavoularies, S. 1989 Measurements of heat diffusion from a continuous line source in a uniformly sheared turbulent flow. *J. Fluid Mech.* **202**, 233–261.

Laufer, J. 1954 The structure of turbulence in fully developed pipe flow. *NACA Tech. Rep.* R 1174.

Launay, K. 1998 Analysis of Lagrangian models for predicting the turbulent particles dispersion and proposal of a model integrating the fluid turbulence experienced by the particle. PhD thesis, Universite Louis Pasteur, Strasbourg.

Lu, Q. Q., Fontaine, J. R. & Aubertin, G. 1993 A Lagrangian model for solid particles in turbulent flows. *Intl J. Multiphase Flow* **19**, 347–367.

Mei, R. 1995 The dispersion of particles with nonlinear drag and history force in homogeneous turbulence. *Proc. 6th Intl Symp on Gas-Solid Flows, Hilton Head Island, S. Carolina, USA* (ed. D. E. Stock, Y. Tsuji, M. W. Reeks, E. E. Michaelides & M. Gautam). ASME FED-vol 228, pp. 411–417.

Mols, B. M. 1999 Particle dispersion and deposition in horizontal turbulent channel and tube flows PhD thesis, Delft Technical University, The Netherlands.

Reeks, M. W. 1991 On a kinetic equation for the transport of particles in turbulent flows. *Phys Fluids* A **3**, 446–456.

Snyder, W. H. & Lumley, J. L. 1971 Some measurements of particle velocity autocorrelation functions in turbulent flow. *J. Fluid Mech.* **48**, 41–71.

Squires, K. D. & Eaton, J. K. 1991 Measurements of particle dispersion obtained from direct numerical simulation of isotropic turbulence. *J. Fluid Mech.* **226**, 1–35.

Stock, D. E. 1996 Particle dispersion in flowing gases – 1994 Freeman Scholar Lecture. *Trans. ASME: J. Fluids Engng* 118, 4–17.

Sundaram, S. & Collins, L. 1999 A numerical study of the modulation of isotropic turbulence by suspended particles. *J. Fluid Mech.* **379**, 105–143.

Tavoularies, S. & Karnik, U. 1989 Further experiments on the evolution of turbulent stresses and scales in uniformly sheared turbulence. *J. Fluid Mech.* **204**, 457–478.

Taylor, G. I. 1921 Diffusion by continuous movements. *Proc. Lond. Math. Soc.* **XX**, 196–212.

Taylor, G. I. 1954 The dispersion of matter in turbulent flow through a pipe. *Proc. R. Soc. Lond.* A **CCXXIII**, 446–468.

Vames, J. T. & Hanratty, T. J. 1988 Turbulent dispersion of droplets for air flow in a pipe. *Exps. Fluids* **6**, 94–104.

Wang, L.-P. & Stock, D. E. 1992 Stochastic trajectory models for turbulence diffusion: Monte Carlo process versus Markov chains. *Atmos. Environ.* **26A**, 1599–1607.

Wells, M. R. & Stock, D. E. 1983 The effects of crossing trajectories on the dispersion of particles in a turbulent flow. *J. Fluid Mech.* **136**, 31–62.